

# Scattering of low energy neutrinos and antineutrinos by neon and argon

Ian B. Whittingham 

*College of Science and Engineering, James Cook University, Townsville, 4811 Queensland, Australia*

 (Received 6 September 2022; accepted 30 November 2022; published 12 December 2022)

The theory of scattering of low energy neutrinos and antineutrinos by atomic electrons has recently been developed [I. B. Whittingham, *Phys. Rev. D* **105**, 013008 (2022)] using the bound interaction picture in configuration space to fully implement the relationship between the neutrino helicities and the orbital and spin angular momenta of the atomic electrons. The energy spectra of ionization electrons produced by scattering of neutrinos and antineutrinos with energies of 5, 10, 20, and 30 keV by hydrogen, helium and neon were calculated using Dirac screened Coulombic eigenfunctions. This paper reports further applications of this theory, to a new calculation of the energy spectra for neon, as the original calculation used some screening constants which underestimated the effects of screening in the inner subshells, and to scattering by argon. The results are presented as ratios to the corresponding quantities for scattering by  $Z$  free electrons. The new spectra ratios for neon are larger than the original ratios by  $\approx 0.03$ – $\approx 0.14$ , with the greatest increases occurring for 10 keV neutrinos and antineutrinos. Integrated spectra ratios range from 0.16 to 0.59 for neon, and from 0.15 to 0.48 for argon, as the neutrino energy increases from 5 to 30 keV.

DOI: [10.1103/PhysRevD.106.113001](https://doi.org/10.1103/PhysRevD.106.113001)

## I. INTRODUCTION

There is significant interest in the low energy O(10 keV) scattering of electron neutrinos and antineutrinos by atomic electrons

$$\nu_e(\bar{\nu}_e) + e^- \rightarrow \nu_e(\bar{\nu}_e) + e^-, \quad (1)$$

for which the binding of the atomic electron cannot be ignored and one can expect modifications of the free electron scattering formulas. One example is the study of possible electromagnetic properties of neutrinos, such as magnetic and electric dipole moments, using low energy scattering of neutrinos and antineutrinos [1,2]. For a review of neutrino-atom collisions, see [3].

Of particular interest is the ionization of atoms by neutrinos and antineutrinos. Ionization cross sections calculated for H, He and Ne were found [4] to be smaller than the corresponding free electron cross sections, and the calculations were then extended [5] to the electron spectra for H, He and Ne, and integrated ionization cross sections for H, He, Ne and Xe.

These calculations treat the  $\nu_e$ -electron scattering process as a probability weighted scattering by a free electron of mass  $\tilde{m}$ , where

$$\tilde{m}^2 = E_{e_i}^2 - \mathbf{p}_{e_i}^2, \quad (2)$$

$E_{e_i} = m_e + \epsilon$  is the energy of the initial bound electron, where  $\epsilon$  is the binding energy, and the momentum  $\mathbf{p}_{e_i}$  is determined by the probability amplitude  $|\Psi_{n_i l_i m_i}(\mathbf{p}_{e_i})|^2$ , where  $\Psi_{n_i l_i m_i}(\mathbf{p}_{e_i})$  is the momentum-space atomic wave function. Spin-independent nonrelativistic atomic wave functions are used for the initial electron and Coulombic effects on the final electron are ignored. These calculations destroy the relationship between the neutrino helicities and the orbital and spin angular momenta of the atomic electrons. Some of these issues have been addressed by [6–8] and their approach is closest in spirit to the present calculations.

The theory of scattering of neutrinos and antineutrinos by bound electrons which maintains the full collision dynamics has recently been developed [9]. The scattering is formulated in configuration space using the bound interaction picture [10,11], rather than the usual formulation in the interaction picture in momentum space as appropriate to scattering by free electrons. The energy spectra of ionization electrons produced by scattering of neutrinos and antineutrinos with energies of 5, 10, 20, and 30 keV by hydrogen, helium and neon were calculated using Dirac screened Coulombic eigenfunctions. The results were significantly different to those of [5] and indicated that binding effects from both the initial bound state and the final continuum state are important.

Very recently, a second quantization formalism has been developed [12] to include atomic effects in the electron

---

*Published by the American Physical Society under the terms of the Creative Commons Attribution 4.0 International license. Further distribution of this work must maintain attribution to the author(s) and the published article's title, journal citation, and DOI. Funded by SCOAP<sup>3</sup>.*

recoil signal for dark matter or neutrino scattering. Although the neutrino scattering amplitude includes more general interactions than the  $W$ - and  $Z$ - exchange of the Standard Model, the formalism treats the atomic electrons as nonrelativistic and includes the electron spin through a nonrelativistic approximation to the four-component Dirac eigenfunction which ignores coupling between the spin and orbital angular momenta.

This paper reports further applications of the bound interaction picture theory [9], to a new calculation of the energy spectra for neon, as the original calculation used some screening constants which underestimated the effects of screening in the inner subshells, and to scattering by argon as it is the basis of current and near-future experiments sensitive to neutrino-electron scattering.

The general formalism for the scattering of neutrinos and antineutrinos by atomic electrons is summarized in Sec. II, and the radial matrix elements which occur in the atomic electron scattering tensor discussed in Sec. III. Results for the energy spectra of the ionization electrons produced in scattering from neon and argon are presented and discussed in Sec. IV, and Sec. V contains a summary and conclusions for the investigation.

## II. GENERAL FORMALISM FOR NEUTRINO SCATTERING BY ATOMIC ELECTRONS

The scattering of neutrinos by atomic electrons involves both  $W$ - and  $Z$ - boson exchange. The total  $S$ -matrix in the bound interaction picture for  $\nu_e$  scattering at low momentum transfers  $k^2 \ll M_A^2$ , where  $A = W, Z$ , is [9]

$$S_{fi}^{(\nu)} = -\pi i \frac{G_F}{\sqrt{2}} \delta(E_{fi}^{(\nu)}) M_{n_f, n_i}^{(e)}(\mathbf{q})^\alpha M^{(\nu)}(\mathbf{p}_{\nu_f}, s_f, \mathbf{p}_{\nu_i}, s_i)_\alpha, \quad (3)$$

where the atomic electron scattering amplitude is

$$M_{n_f, n_i}^{(e)}(\mathbf{q})^\alpha = \int d^3x e^{i(\mathbf{p}_{\nu_i} - \mathbf{p}_{\nu_f}) \cdot \mathbf{x}} \times \bar{\phi}_{n_f}^{(+)}(\mathbf{x}) \gamma^\alpha (\bar{v}_e + \bar{a}_e \gamma_5) \phi_{n_i}^{(+)}(\mathbf{x}), \quad (4)$$

the quantity

$$\delta(E_{fi}^{(\nu)}) \equiv \delta(E_{n_f} + E_{\nu_f} - E_{n_i} - E_{\nu_i}). \quad (5)$$

incorporates energy conservation,  $\mathbf{q} = \mathbf{p}_{\nu_i} - \mathbf{p}_{\nu_f}$  is the momentum transfer from the neutrino, and

$$M^{(\nu)}(\mathbf{p}_{\nu_f}, s_f, \mathbf{p}_{\nu_i}, s_i)_\alpha = \bar{u}^{(s_f)}(\mathbf{p}_{\nu_f}) \gamma_\alpha (1 - \gamma_5) u^{(s_i)}(\mathbf{p}_{\nu_i}) \quad (6)$$

is the neutrino scattering amplitude. Here  $\phi_n^{(+)}(\mathbf{x})$  is the positive energy eigenfunction for an electron in a state of the external field  $A^{(\text{ext})}$  specified by the quantum numbers

$n$ , and  $u^{(s)}(\mathbf{p}_\nu)$  are the plane wave spinors describing a neutrino with momentum  $\mathbf{p}_\nu$  and helicity  $s$ . The natural unit system  $\hbar = c = 1$  is used throughout, the scalar product of two 4-vectors is  $A \cdot B \equiv g^{\alpha\beta} A_\alpha B_\beta = A_0 B_0 - \mathbf{A} \cdot \mathbf{B}$ , the Dirac matrices  $\gamma^\alpha$ , ( $\alpha = 0, 1, 2, 3$ ) satisfy  $\{\gamma^\alpha, \gamma^\beta\} = 2g^{\alpha\beta}$ , and  $\gamma_5 \equiv i\gamma^0 \gamma^1 \gamma^2 \gamma^3$ .

The electron mixing parameters are

$$\bar{v}_e = v_e + 2, \quad \bar{a}_e = a_e - 2, \quad (7)$$

where

$$v_e = -1 + 4\sin^2\theta_W, \quad a_e = 1, \quad (8)$$

and  $\theta_W$  is the weak mixing angle.

For scattering of antineutrinos,  $M^{(\nu)}$  is replaced by

$$M^{(\bar{\nu})}(\mathbf{p}_{\nu_f}, s_f, \mathbf{p}_{\nu_i}, s_i)_\alpha = \bar{v}^{(s_i)}(\mathbf{p}_{\nu_i}) \gamma_\alpha (1 - \gamma_5) v^{(s_f)}(\mathbf{p}_{\nu_f}), \quad (9)$$

where  $v^{(s)}(\mathbf{p}_\nu)$  is the antineutrino plane wave spinor, and  $\delta(E_{fi}^{(\nu)})$  is replaced by  $\delta(E_{fi}^{(\bar{\nu})})$ .

We assume the atomic electron moves in a spherically symmetric potential  $V(r) = eA^{(\text{ext})}(r)$ , for which the Dirac equation has eigenfunctions of the form [13]

$$\phi_{\kappa, \mu, E}(r, \theta, \varphi) = \frac{1}{r} \begin{pmatrix} g_{\kappa, E}(r) \chi_\kappa^\mu(\Omega) \\ i f_{\kappa, E}(r) \chi_{-\kappa}^\mu(\Omega) \end{pmatrix}, \quad (10)$$

where  $(r, \theta, \varphi) = (r, \Omega)$  are spherical polar coordinates, and  $\chi_\kappa^\mu(\Omega)$  are the spinor spherical harmonics

$$\chi_\kappa^\mu(\Omega) = \sum_{m_s} C\left(l_\kappa, \frac{1}{2}, j, \mu - m_s, m_s, \mu\right) Y_{l_\kappa}^{\mu - m_s}(\Omega) \chi_{m_s}. \quad (11)$$

Here  $C(j_1, j_2, j_3, m_1, m_2, m_3)$  is a Clebsch-Gordon coefficient, and  $\chi_{m_s}$  are the two component Pauli spinors. The total angular momentum  $j$  and orbital angular momentum  $l_\kappa$  are obtained from the quantum number  $\kappa$  by

$$j = |\kappa| - \frac{1}{2}, \quad l_\kappa = \begin{cases} \kappa & \kappa > 0 \\ -\kappa - 1 & \kappa < 0 \end{cases}, \quad l_{-\kappa} = l_\kappa - \frac{\kappa}{|\kappa|}, \quad (12)$$

where  $\kappa$  takes all nonzero integral values. The radial functions satisfy

$$\begin{pmatrix} d/dr + \kappa/r & -(E + m_e - V(r)) \\ E - m_e - V(r) & d/dr - \kappa/r \end{pmatrix} \begin{pmatrix} g_{\kappa, E}(r) \\ f_{\kappa, E}(r) \end{pmatrix} = 0. \quad (13)$$

The energy spectrum of the ionized electrons is [9]

$$\frac{d\sigma^{(\nu)}}{dE_f} = \frac{G_F^2}{8\pi} \frac{1}{16m_e E_{\nu_i}^2} \int d^3q^2 L_{fi}(\tilde{\mathbf{q}}, p_{\nu_i}, p_{\nu_f}), \quad (14)$$

where

$$\begin{aligned} L_{fi}(\tilde{\mathbf{q}}, p_{\nu_i}, p_{\nu_f}) &= \text{Re}[L_{fi}^{(e)}(\tilde{\mathbf{q}})^{\beta\alpha}] \text{Re}[L^{(\nu)}(p_{\nu_i}, p_{\nu_f})_{\beta\alpha}] \\ &\quad - \text{Im}[L_{fi}^{(e)}(\tilde{\mathbf{q}})^{\beta\alpha}] \text{Im}[L^{(\nu)}(p_{\nu_i}, p_{\nu_f})_{\beta\alpha}] \end{aligned} \quad (15)$$

and it is understood that  $E_{\nu_f} = E_i + E_{\nu_i} - E_f$ . The neutrino scattering tensor is

$$\begin{aligned} L^{(\nu)}(p_{\nu_i}, p_{\nu_f})^{\beta\alpha} &\equiv [\bar{u}^{(s_f)}(\mathbf{p}_{\nu_f})\gamma^\beta(1-\gamma_5)u^{(s_i)}(\mathbf{p}_{\nu_i})]^\dagger \\ &\quad \times \bar{u}^{(s_f)}(\mathbf{p}_{\nu_f})\gamma^\alpha(1-\gamma_5)u^{(s_i)}(\mathbf{p}_{\nu_i}) \\ &= 8(p_{\nu_i}^\beta p_{\nu_f}^\alpha + p_{\nu_i}^\alpha p_{\nu_f}^\beta - p_{\nu_i} \cdot p_{\nu_f} g^{\beta\alpha} \\ &\quad + ie^{\rho\beta\lambda\alpha} p_{\nu_i\rho} p_{\nu_f\lambda}), \end{aligned} \quad (16)$$

where  $s_i = s_f = -1/2$ . The atomic electron scattering tensor is

$$\begin{aligned} L_{fi}^{(e)}(\tilde{\mathbf{q}})^{\beta\alpha} &= \sum_{\kappa_f, \bar{l}, l} i^{l-\bar{l}} (2\bar{l}+1)(2l+1) [\bar{v}_e^2 L_{v_e v_e}^{\beta\alpha} \\ &\quad + \bar{a}_e^2 L_{a_e a_e}^{\beta\alpha} + \bar{v}_e \bar{a}_e (L_{v_e a_e}^{\beta\alpha} + L_{a_e v_e}^{\beta\alpha})], \end{aligned} \quad (17)$$

where  $\tilde{\mathbf{q}} \equiv (0, 0, q)$  and  $q \equiv |\mathbf{q}|$ . The quantities  $L_{v_e v_e}^{\beta\alpha}$ , etc involve [9] various angular momentum coupling coefficients and the radial integrals

$$\begin{aligned} I_i^{gg}(q) &\equiv \int dr g_{\kappa_f, E_f}^*(r) j_l(qr) g_{\kappa_i, E_i}(r), \\ I_i^{gf}(q) &\equiv \int dr g_{\kappa_f, E_f}^*(r) j_l(qr) f_{\kappa_i, E_i}(r), \\ I_i^{fg}(q) &\equiv \int dr f_{\kappa_f, E_f}^*(r) j_l(qr) g_{\kappa_i, E_i}(r), \\ I_i^{ff}(q) &\equiv \int dr f_{\kappa_f, E_f}^*(r) j_l(qr) f_{\kappa_i, E_i}(r). \end{aligned} \quad (18)$$

The scattering of antineutrinos involves

$$\begin{aligned} L^{(\bar{\nu})}(p_{\nu_i}, p_{\nu_f})^{\beta\alpha} &\equiv [\bar{v}^{(s_i)}(\mathbf{p}_{\nu_i})\gamma^\beta(1-\gamma_5)v^{(s_f)}(\mathbf{p}_{\nu_f})]^\dagger \\ &\quad \times \bar{v}^{(s_i)}(\mathbf{p}_{\nu_i})\gamma^\alpha(1-\gamma_5)v^{(s_f)}(\mathbf{p}_{\nu_f}) \\ &= L^{(\nu)}(-p_{\nu_f}, -p_{\nu_i})^{\beta\alpha}, \\ &= [L^{(\nu)}(p_{\nu_i}, p_{\nu_f})^{\beta\alpha}]^*, \end{aligned} \quad (19)$$

where  $v^{(s)}(\mathbf{p}_\nu)$  is the antineutrino plane wave spinor, and  $s_i = s_f = +1/2$ .

### III. RADIAL MATRIX ELEMENTS

The radial integrals (18) involve the Dirac radial functions  $g_{\kappa, E}(r)$  and  $f_{\kappa, E}(r)$  for the initial bound electron and the final continuum electron. We assume a potential of a Coulombic form  $V(r) = -\alpha Z_{\text{eff}}/r$ , where  $Z_{\text{eff}}$  is an effective nuclear charge. The radial Dirac equations (13) then have analytic solutions [13] in terms of confluent hypergeometric functions  ${}_1F_1(a, c, z)$ .

As scattering by electrons in the ground states of Ne and Ar involve only K-, L- and M- shell electrons, we can use the simplified expressions [13,14]

$$\begin{aligned} \begin{pmatrix} g_{\kappa_i, E_i}(r) \\ f_{\kappa_i, E_i}(r) \end{pmatrix} &= N_i \begin{pmatrix} \sqrt{m_e + E_i} \\ -\sqrt{m_e - E_i} \end{pmatrix} (2\lambda_i r)^{\gamma_i} e^{-\lambda_i r} \\ &\quad \times \left[ \begin{pmatrix} c_0 \\ a_0 \end{pmatrix} + \begin{pmatrix} c_1 \\ a_1 \end{pmatrix} \lambda_i r + \begin{pmatrix} c_2 \\ a_2 \end{pmatrix} (\lambda_i r)^2 \right] \end{aligned} \quad (20)$$

where

$$\lambda_i \equiv \sqrt{m_e^2 - E_i^2}, \quad \gamma_i \equiv \sqrt{\kappa_i^2 - \zeta^2}, \quad \zeta \equiv \alpha Z_{\text{eff}}, \quad (21)$$

and the initial state energy  $E_i$  is

$$E_{n, \kappa_i} = m_e \left[ 1 + \left( \frac{\zeta}{n - |\kappa_i| + \gamma_i} \right)^2 \right]^{-1/2}. \quad (22)$$

The dimensionless coefficients  $(c_i, a_i, N_i)$  for the K-shell ( $n = 1, \kappa_i = -1$ ), L<sub>I</sub>-ubshell ( $n = 2, \kappa_i = -1$ ), L<sub>II</sub>-subshell ( $n = 2, \kappa_i = +1$ ), L<sub>III</sub>-subshell ( $n = 2, \kappa_i = -2$ ), M<sub>I</sub>-subshell ( $n = 3, \kappa_i = -1$ ), M<sub>II</sub>-subshell ( $n = 3, \kappa_i = +1$ ), and M<sub>III</sub>-subshell ( $n = 3, \kappa_i = -2$ ) are listed in Table I.

The screening effects of the electrons in the filled K- shell, L-subshells and M-subshells are represented by an effective nuclear charge of the form  $Z_{\text{eff}} = Z - s_i$ , a procedure that should be reasonable for small principal quantum number  $n$  and small  $n - l$  [15]. These screening constants  $s_i$  are taken from the fits [16] of Dirac single electron eigenfunctions to empirical binding energies. For neon, they are 2.016 (K-shell), 6.254 (L<sub>I</sub>-subshell), and 7.482 (L<sub>II</sub>- and L<sub>III</sub>-subshells). For argon, the constants are 2.721 (K-shell), 8.248 (L<sub>I</sub>-subshell), 9.470 (L<sub>II</sub>- and L<sub>III</sub>-subshells), 13.603 (M<sub>I</sub>-subshell), and 14.771 (M<sub>II</sub>- and M<sub>III</sub>-subshells).

The final electron continuum states involve the hypergeometric function  ${}_1F_1(a, c, z)$  where  $a = \gamma_f + 1 + iy$ ,  $c = 2\gamma_f + 1$ ,  $z = 2ip_f r$ , and

$$\gamma_f \equiv \sqrt{\kappa_f^2 - \zeta^2}, \quad p_f \equiv \sqrt{E_f^2 - m_e^2}, \quad y \equiv \frac{\zeta E_f}{p_f}. \quad (23)$$

TABLE I. Parameters defining the K-, L- and M-shell Coulombic radial eigenfunctions for Ne and Ar, expressed in terms of  $\zeta = \alpha Z$  and  $\gamma = \sqrt{\kappa^2 - \zeta^2}$ .

Subshell	$E_{nk}$	$\lambda$	$N_i$	$a_0$	$c_0$	$a_1$	$c_1$	$a_2$	$c_2$
$K$	$\gamma$	$\zeta$	$\left(\frac{\zeta}{\Gamma(2\gamma+1)}\right)^{1/2}$	1	1	0	0	0	0
$L_I$	$\left(\frac{\gamma+1}{2}\right)^{1/2}$	$\frac{\zeta}{2E}$	$\frac{1}{2} \left[ \frac{\lambda(2\gamma+1)}{E(2E+1)\Gamma(2\gamma+1)} \right]^{1/2}$	$2(E+1)$	$2E$	$-2\left(\frac{2E+1}{2\gamma+1}\right)$	$-2\left(\frac{2E+1}{2\gamma+1}\right)$	0	0
$L_{II}$	$\left(\frac{\gamma+1}{2}\right)^{1/2}$	$\frac{\zeta}{2E}$	$\frac{1}{2} \left[ \frac{\lambda(2\gamma+1)}{E(2E-1)\Gamma(2\gamma+1)} \right]^{1/2}$	$2E$	$2(E-1)$	$-2\left(\frac{2E-1}{2\gamma+1}\right)$	$-2\left(\frac{2E-1}{2\gamma+1}\right)$	0	0
$L_{III}$	$\frac{\gamma}{2}$	$\frac{\zeta}{2}$	$\left(\frac{\lambda}{\Gamma(2\gamma+1)}\right)^{1/2}$	1	1	0	0	0	0
$M_I$	$\frac{\gamma+2}{\sqrt{4\gamma+5}}$	$\frac{\zeta}{\sqrt{4\gamma+5}}$	$\lambda \left[ \frac{\lambda(\gamma+1)(2\gamma+1)}{2\zeta(\zeta+\lambda)\Gamma(2\gamma+1)} \right]^{1/2}$	$3 + \frac{\zeta}{\lambda}$	$-1 + \frac{\zeta}{\lambda}$	$-\frac{4}{2\gamma+1} \left(2 + \frac{\zeta}{\lambda}\right)$	$-\frac{4\zeta}{\lambda(2\gamma+1)}$	$\frac{2}{(\gamma+1)(2\gamma+1)} \left(1 + \frac{\zeta}{\lambda}\right)$	$a_2$
$M_{II}$	$\frac{\gamma+2}{\sqrt{4\gamma+5}}$	$\frac{\zeta}{\sqrt{4\gamma+5}}$	$\lambda \left[ \frac{\lambda(\gamma+1)(2\gamma+1)}{2\zeta(\zeta-\lambda)\Gamma(2\gamma+1)} \right]^{1/2}$	$1 + \frac{\zeta}{\lambda}$	$-3 + \frac{\zeta}{\lambda}$	$-\frac{4\zeta}{\lambda(2\gamma+1)}$	$\frac{4}{2\gamma+1} \left(2 - \frac{\zeta}{\lambda}\right)$	$-\frac{2}{(\gamma+1)(2\gamma+1)} \left(1 - \frac{\zeta}{\lambda}\right)$	$a_2$
$M_{III}$	$\frac{\gamma+1}{\sqrt{2\gamma+5}}$	$\frac{\zeta}{\sqrt{2\gamma+5}}$	$\lambda \left[ \frac{\lambda(2\gamma+1)}{2\zeta(\zeta+2\lambda)\Gamma(2\gamma+1)} \right]^{1/2}$	$3 + \frac{\zeta}{\lambda}$	$1 + \frac{\zeta}{\lambda}$	$-\frac{2}{2\gamma+1} \left(2 + \frac{\zeta}{\lambda}\right)$	$-\frac{2}{2\gamma+1} \left(2 + \frac{\zeta}{\lambda}\right)$	0	0

We choose to integrate the Dirac equation directly to obtain the continuum states rather than evaluate the hypergeometric functions as  $a$  and  $z$  are complex and the computation of  ${}_1F_1(a, c, z)$  would involve the summation of a slowly convergent complex series for each required value of  $z$ . For each shell and subshell calculation, the continuum state electrons are assumed to move in the same potential as the bound state electrons [17].

#### IV. RESULTS AND DISCUSSION

The energy spectra  $d\sigma/dE_f$  of the ionization electrons have been calculated as a function of the electron kinetic energy  $\epsilon_f = E_f - m_e$ . Results are obtained for scattering of 5, 10, 20, and 30 keV neutrino energies by the ground state systems Ne( $1s^2 2s^2 2p^6$ ) and Ar( $1s^2 2s^2 2p^6 3s^2 3p^6$ ), where the electrons are considered as independent scattering centers.

The energy spectra are compared to those for scattering from free electrons, for which [4]

$$\left(\frac{d\sigma^{(\nu)}}{dE_f}\right)_{(\text{Free})} = \frac{G_F^2 m_e}{8\pi E_{\nu_i}^2} \{ (\bar{v}_e - \bar{a}_e)^2 E_{\nu_i}^2 + (\bar{v}_e + \bar{a}_e)^2 (E_{\nu_i} + m_e - E_f)^2 + m_e (\bar{v}_e^2 - \bar{a}_e^2) (m_e - E_f) \}, \quad (24)$$

where  $m_e \leq E_f \leq m_e + \epsilon_f^{\max}$  and the maximum kinetic energy is

$$\epsilon_f^{\max} = \frac{2E_{\nu_i}^2}{m_e + 2E_{\nu_i}}. \quad (25)$$

The total cross section for scattering off free electrons is [4]

$$\sigma_{(\text{Free})}^{(\nu)} = \frac{G_F^2 m_e E_{\nu_i}}{8\pi} \left[ (\bar{v}_e - \bar{a}_e)^2 \frac{2E_{\nu_i}}{m_e + 2E_{\nu_i}} + \frac{1}{3} (\bar{v}_e + \bar{a}_e)^2 \left\{ 1 - \frac{m_e^3}{(m_e + 2E_{\nu_i})^3} \right\} - (\bar{v}_e^2 - \bar{a}_e^2) \frac{2m_e E_{\nu_i}}{(m_e + 2E_{\nu_i})^2} \right]. \quad (26)$$

The expressions for  $\bar{v}_e$  scattering can be obtained by the interchange  $\bar{a}_e \leftrightarrow -\bar{a}_e$  in (24) and (26).

Results for  $\nu_e$  and  $\bar{\nu}_e$  scattering by Ne are given in Table II, and by Ar in Table III. The energy spectra and cross sections are expressed as ratios

$$R^{(\nu)}(E_f) = \frac{d\sigma^{(\nu)}/dE_f}{Z(d\sigma^{(\nu)}/dE_f)_{(\text{Free})}}, \quad (27)$$

and  $\sigma^{(\nu)}/Z\sigma_{(\text{Free})}^{(\nu)}$ , to the corresponding quantities for scattering by  $Z$  free electrons. Tables and plots of the energy spectra for scattering from free electrons are given in [9].

The energy spectra ratios for scattering of neutrinos by Ne and Ar are shown in Figs. 1 and 2 respectively. Plots for scattering of antineutrinos are not shown as they differ only very slightly from those for scattering by neutrinos. The energy spectra ratios become constant at low kinetic energies and can safely be extrapolated to lower kinetic energies.

The present spectra for Ne have the same general form as those calculated in [5], but have a much smoother structure and are significantly lower, representing a stronger dependence on atomic binding effects.

The largest binding energy of 3.2059 keV, for the K-shell of argon, is less than the lowest incident neutrino energy of  $E_{\nu_i} = 5$  keV considered in the present calculations.

TABLE II. Energy spectra  $d\sigma^{(\nu)}/dE_f$  of the ionization electrons from scattering of incident neutrinos of energy  $E_{\nu_i}$  by neon. The results are expressed as ratios to the spectra  $10(d\sigma^{(\nu)}/dE_f)_{(\text{Free})}$  for scattering by 10 free electrons and are given as a function of the kinetic energy  $\epsilon_f$  of the electron. Also shown are the integrated spectra  $\sigma^{(\nu)}$  expressed as a ratio to the integrated spectra  $10\sigma^{(\nu)}_{(\text{Free})}$  for 10 free electrons. Results for scattering of antineutrinos are given in parentheses.

$\epsilon_f/\epsilon_f^{\text{max}}$	$E_{\nu_i} = 5$ (keV)	$E_{\nu_i} = 10$ (keV)	$E_{\nu_i} = 20$ (keV)	$E_{\nu_i} = 30$ (keV)
0.01	0.2175 (0.2134)	0.3867 (0.3821)	0.4977 (0.4882)	0.5720 (0.5578)
0.1	0.2041 (0.2004)	0.3943 (0.3896)	0.5258 (0.5171)	0.6155 (0.6020)
0.2	0.1880 (0.1848)	0.3983 (0.3933)	0.5358 (0.5282)	0.6272 (0.6148)
0.3	0.1716 (0.1690)	0.3982 (0.3929)	0.5383 (0.5320)	0.6287 (0.6187)
0.4	0.1566 (0.1546)	0.3930 (0.3876)	0.5370 (0.5321)	0.6249 (0.6168)
0.5	0.1444 (0.1430)	0.3794 (0.3745)	0.5330 (0.5296)	0.6170 (0.6121)
0.6	0.1359 (0.1350)	0.3524 (0.3490)	0.5264 (0.5245)	0.6055 (0.6044)
0.7	0.1305 (0.1302)	0.3102 (0.3093)	0.5140 (0.5139)	0.5901 (0.5934)
0.8	0.1263 (0.1268)	0.2636 (0.2655)	0.4750 (0.4788)	0.5666 (0.5748)
0.9	0.1210 (0.1226)	0.2300 (0.2347)	0.3710 (0.3815)	0.4792 (0.4957)
1.0	0.1136 (0.1166)	0.2021 (0.2108)	0.2745 (0.2922)	0.3051 (0.3302)
$\epsilon_f^{\text{max}}$ (eV)	95.969	376.65	1451.9	3152.4
$\sigma^{(\nu)}/\sigma^{(\nu)}_{(\text{Free})}$	0.1612 (0.1600)	0.3549 (0.3540)	0.5051 (0.5050)	0.5910 (0.5909)

TABLE III. Energy spectra  $d\sigma^{(\nu)}/dE_f$  of the ionization electrons from scattering of incident neutrinos of energy  $E_{\nu_i}$  by argon. The results are expressed as ratios to the spectra  $18(d\sigma^{(\nu)}/dE_f)_{(\text{Free})}$  for scattering by 18 free electrons and are given as a function of the kinetic energy  $\epsilon_f$  of the electron. Also shown are the integrated spectra  $\sigma^{(\nu)}$  expressed as a ratio to the integrated spectra  $18\sigma^{(\nu)}_{(\text{Free})}$  for 18 free electrons. Results for scattering of antineutrinos are given in parentheses.

$\epsilon_f/\epsilon_f^{\text{max}}$	$E_{\nu_i} = 5$ (keV)	$E_{\nu_i} = 10$ (keV)	$E_{\nu_i} = 20$ (keV)	$E_{\nu_i} = 30$ (keV)
0.01	0.1867 (0.1845)	0.2855 (0.2813)	0.4318 (0.4228)	0.4964 (0.4859)
0.1	0.1875 (0.1851)	0.2929 (0.2888)	0.4493 (0.4404)	0.5223 (0.5124)
0.2	0.1856 (0.1830)	0.2945 (0.2907)	0.4502 (0.4417)	0.5275 (0.5183)
0.3	0.1792 (0.1767)	0.2929 (0.2894)	0.4451 (0.4374)	0.5256 (0.5171)
0.4	0.1669 (0.1647)	0.2890 (0.2861)	0.4361 (0.4297)	0.5169 (0.5095)
0.5	0.1493 (0.1478)	0.2842 (0.2818)	0.4240 (0.4192)	0.5007 (0.4948)
0.6	0.1311 (0.1301)	0.2801 (0.2781)	0.4096 (0.4069)	0.4756 (0.4726)
0.7	0.1170 (0.1166)	0.2712 (0.2699)	0.3917 (0.3918)	0.4419 (0.4429)
0.8	0.1067 (0.1068)	0.2352 (0.2360)	0.3693 (0.3730)	0.4002 (0.4065)
0.9	0.09465 (0.09562)	0.1865 (0.1898)	0.3251 (0.3339)	0.3494 (0.3630)
1.0	0.07822 (0.08011)	0.1499 (0.1559)	0.2164 (0.2316)	0.2220 (0.2449)
$\epsilon_f^{\text{max}}$ (eV)	95.969	376.65	1451.9	3152.4
$\sigma^{(\bar{\nu})}/\sigma^{(\bar{\nu})}_{(\text{Free})}$	0.1533 (0.1524)	0.2730 (0.2719)	0.4138 (0.4128)	0.4779 (0.4799)

Consequently, all occupied shells and subshells contribute to the energy spectra although, for the lower neutrino energies, the contributions from the inner shell and subshells will be small. For neon, the K-shell contributions at 5 keV and 10 keV are only  $O(10^{-3})$  and  $O(10^{-2})$  respectively. At all neutrino energies, the  $L_I$  subshell gives the largest contribution, and the  $L_{II}$  and  $L_{III}$  contributions are quite similar. For argon, the K-shell contributions at 5 keV and 10 keV are  $O(10^{-5})$  and  $O(10^{-3})$  respectively, and the L-subshell contributions at 5 keV are  $O(10^{-2})$ . The  $M_I$  subshell contribution is dominant at all energies, the  $L_{II}$  and  $L_{III}$  contributions are similar, as are the  $M_{II}$  and  $M_{III}$  contributions.

The major computational challenge is to obtain satisfactory convergence in the sum over  $\kappa_f$ , as the convergence decreases with increasing  $\epsilon_f$ . The imposed practical limit  $|\kappa_f| \leq 50$  ensured the fractional contributions of the neglected terms were less than  $1 \times 10^{-4}$  for  $\epsilon_f \lesssim 1.4$  keV in the Ne spectra, and for  $\epsilon_f \lesssim 0.6$  keV in the Ne spectra. However, for the higher energies, the convergence decreased and the contributions of the neglected terms increased to  $1 \times 10^{-3}$  for the L subshells of Ne, and  $1 \times 10^{-2}$  for the M subshells of Ar, so the numbers shown for these higher energies are slight underestimates.

The binding effects in the spectra increase with atomic number, decrease with increasing  $E_{\nu_i}$  and, for each  $E_{\nu_i}$ , are

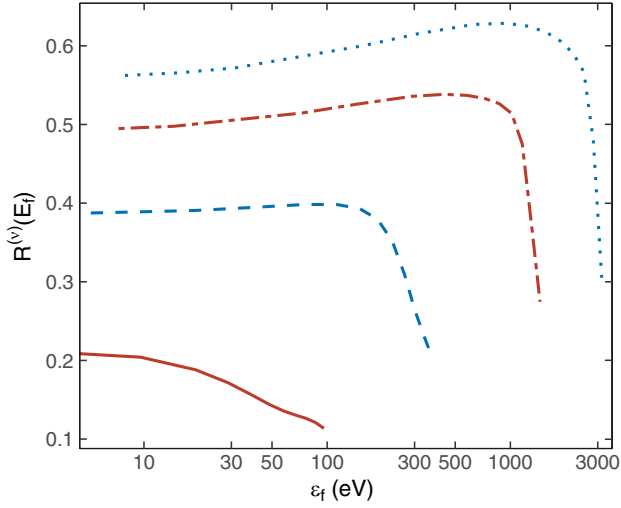


FIG. 1. Energy spectra ratios  $R^{(\nu)}(E_f)$  [Eq. (27)], as a function of electron kinetic energy  $\epsilon_f$ , of ionization electrons resulting from scattering of neutrinos by ground state neon. Results are shown for scattering of 5 keV (solid line), 10 keV (dashed line), 20 keV (dash-dotted line), and 30 keV (dotted line) incident neutrino energies.

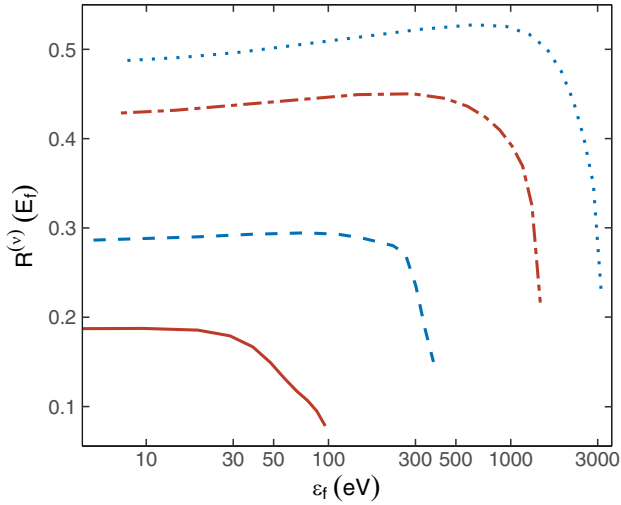


FIG. 2. Energy spectra ratios  $R^{(\nu)}(E_f)$  [Eq. (27)], as a function of electron kinetic energy  $\epsilon_f$ , of ionization electrons resulting from scattering of neutrinos by ground state argon. Results are shown for scattering of 5 keV (solid line), 10 keV (dashed line), 20 keV (dash-dotted line), and 30 keV (dotted line) incident neutrino energies.

most significant at the high electron energy end of the spectrum. The sharp decrease in the spectra at the high energy end is due to the minimization of the range  $2E_{\nu_f}$  of the  $q^2$  integration in (14) at  $E_f^{\max}$ . Also, for this region,  $q \approx E_{\nu_i}$ , so that the high energy tail will increase as  $E_{\nu_i}$  increases.

The integrated cross sections

$$\sigma^{(\nu)} = \int_{E_l}^{E_u} dE_f \frac{d\sigma^{(\nu)}}{dE_f}, \quad (28)$$

where  $E_l = m_e$  and  $E_u = m_e + \epsilon_f^{\max}$ , can be estimated from the calculated energy spectra. We assume the spectra at  $E_f = m_e$  are the same as at  $m_e + 0.01\epsilon_f^{\max}$ . These integrated cross sections are given in the tables, expressed as ratios to the integrated cross sections  $Z\sigma_{(\text{Free})}^{(\nu)}$  [Eq. (26)] for  $Z$  free electrons.

## V. SUMMARY AND CONCLUSIONS

The recently developed [9] theory of scattering of low energy neutrinos and antineutrinos by atomic electrons, which uses the bound interaction picture in configuration space to fully implement the relationship between the neutrino helicities and the orbital and spin angular momenta of the atomic electrons, has been applied here to the scattering by the ground state systems  $\text{Ne}(1s^2 2s^2 2p^6)$  and  $\text{Ar}(1s^2 2s^2 2p^6 3s^2 3p^6)$ .

The energy spectra  $d\sigma/dE_f$  of the ionization electrons produced in the scattering of electron neutrinos and antineutrinos with energies 5, 10, 20 and 30 keV have been calculated. Results are also obtained for the integrated cross sections. Screened point-Coulomb radial eigenfunctions have been used, with the continuum state eigenfunctions calculated by direct integration of the Dirac equations. The results here for Ne replace those given in [9] which were calculated using some screening constants which underestimated the effects of screening in the inner subshells. The new spectra ratios for neon are larger than the original ratios by  $\approx 0.03$  to  $\approx 0.14$ , with the greatest increases occurring at  $E_{\nu_i} = 10$  keV.

The calculated energy spectra show that binding effects increase with atomic number, decrease with increasing  $E_{\nu_i}$  and, for each  $E_{\nu_i}$ , are greatest at the high electron energy end of the spectrum. The neutrino and antineutrino energy spectra are very similar, with small difference of  $\lesssim 1\%$ .

Binding effects are still very significant at  $E_{\nu_i} = 30$  keV, the integrated spectra ratios being  $\lesssim 0.6$  and  $\lesssim 0.5$  for Ne and Ar respectively. Extension of the calculations to higher neutrino energies to study the further decrease of binding effects would require a substantial increase in the maximum value of  $|\kappa_f|$  used as the  $\kappa_f$  convergence is very slow at higher energies, which is not practical.

The largest uncertainty in the present calculations arises from the choice of the potential  $V(r)$  for the atomic electron, and the consequent form of the radial functions  $g(r)$  and  $f(r)$  used in the evaluation of the radial matrix elements (18). The choice of a Coulombic potential with an effective nuclear charge  $Z_{\text{eff}} = Z - s_i$  to account for electron screening effects is convenient and should be accurate for the small values of  $n$  and  $n - l$  occurring in the

ground states of neon and argon [15]. However, if increased accuracy is required, or extension to, for example, xenon is considered, then self-consistent relativistic radial eigenfunctions [18,19] would be needed.

Relativistic self-consistent field theory includes [18] the effects of magnetic interactions between electrons and retardation of the inter-electronic Coulomb repulsion, as described by the Breit operator. This operator is treated as a first order perturbation to an unperturbed Hamiltonian which is a sum of the Dirac central field Coulombic Hamiltonians for each electron and the total Coulombic inter-electronic interaction. The magnetic and retardation terms are of order  $(v/c)^2$  compared to the interelectronic repulsion term, which is of order  $(\alpha^2 Z)m_e c^2$ . Their contribution is therefore of order  $(\alpha^4 Z^3)m_e c^2$  and increases strongly with  $Z$ . Detailed calculations are discussed in Sec. 7.2 of [14].

The scattering of dark matter (DM) particles by atomic electrons is a promising method for detecting the particles forming the DM component of the Milky Way, and the theoretical treatment of this process shares many features with that for neutrino scattering by atomic electrons. The response of argon and xenon targets has been studied by [20] by treating the atomic electrons and DM particle as nonrelativistic, with a general interaction constructed to satisfy Galilean and rotational invariance. The DarkSide-50

experiment [21] uses an argon target and they have presented a nonrelativistic analysis for a vector mediator based upon atomic and DM form factors. The conversion of a sterile neutrino DM particle into an active neutrino via inelastic scattering with an atomic electron has been considered by [12] using a nonrelativistic second quantization formalism based upon a four-fermion coupling and a mediator which could be scalar, pseudoscalar, vector or axial vector.

The formalism developed in [9], which considers only vector and axial vector couplings, could be readily adapted to the  $Z$ -mediated scattering of a fermionic WIMP DM particle such as the neutralino  $\chi$ . The neutrino scattering tensor  $L_{\beta\alpha}^{(\nu)}$  would be replaced by the appropriate tensor  $L_{\beta\alpha}^{(\chi)}$  for the neutralino, the admixture of vector and axial vector contributions altered to accommodate the neutralino couplings, and changes made to the normalization factors for the plane wave spinors. Generalization to scalar and pseudo-scalar couplings is possible but would require substantial modifications to the formalism, especially to the angular momentum matrix elements.

## ACKNOWLEDGMENTS

The author would like to thank Michael Meehan for assistance with the figures.

- 
- [1] C. Giunti and A. Studenikin, Neutrino electromagnetic interactions: A window to new physics, *Rev. Mod. Phys.* **87**, 531 (2015).
  - [2] J. Jeong, J. E. Kim, and S. Youn, Electromagnetic properties of neutrinos from scattering on bound electrons in atoms, *Int. J. Mod. Phys A* **36**, 2150182 (2021).
  - [3] K. A. Kouzakov and A. I. Studenikin, Theory of neutrino-atom collisions: The history, present status, and BSM physics, *Adv. High Energy Phys.* **2014**, 1 (2014).
  - [4] G. J. Gounaris, E. A. Paschos, and P. I. Porfyriadis, The ionization of H, He or Ne atoms using neutrinos or antineutrinos at keV energies, *Phys. Lett. B* **525**, 63 (2002).
  - [5] G. J. Gounaris, E. A. Paschos, and P. I. Porfyriadis, Electron spectra in the ionization of atoms by neutrinos, *Phys. Rev. D* **70**, 113008 (2004).
  - [6] J.-W. Chen, H.-C. Chi, K.-N. Huang, C.-P. Liu, H.-T. Shiao, L. Singh, H. T. Wong, C.-L. Wu, and C.-P. Wu, Atomic ionization of germanium by neutrinos from ab initio approach, *Phys. Lett. B* **731**, 159 (2014).
  - [7] Jiunn-Wei Chen, Hsin-Chang Chi, Keh-Ning Huang, Hau Bin Li, C.-P. Liu, Lakhwinder Singh, Henry T. Wong, Chih-Liang Wu, and Chih-Pan Wu, Constraining neutrino electromagnetic properties by germanium detectors, *Phys. Rev. D* **91**, 013005 (2015).
  - [8] Jiunn-Wei Chen, Hsin-Chang Chi, C.-P. Liu, and Chih-Pan Wu, Low energy electronic recoil in xenon detectors by solar neutrinos, *Phys. Lett. B* **774**, 656 (2017).
  - [9] I. B. Whittingham, Scattering of low energy neutrinos and antineutrinos by atomic electrons, *Phys. Rev. D* **105**, 013008 (2022).
  - [10] W. H. Furry, On bound states and scattering in positron theory, *Phys. Rev.* **81**, 115 (1951).
  - [11] I. B. Whittingham, Incoherent scattering of gamma rays in heavy atoms, *J. Phys. A* **4**, 21 (1971).
  - [12] Shao-Feng Ge, Pedro Pasquini, and Jie Sheng, Solar active-sterile neutrino conversion with atomic effects at dark matter direct detection experiments, *J. High Energy Phys.* **05** (2022) 088.
  - [13] M. E. Rose, *Relativistic Electron Theory* (Wiley, New York, 1961).
  - [14] T. P. Das, *Relativistic Quantum Mechanics of Electrons* (Harper & Row, New York, 1973).
  - [15] H. A. Bethe and E. E. Salpeter, *Quantum Mechanics of One- and Two- Electron Atoms* (Springer-Verlag, Berlin, 1957).
  - [16] D. Thomas, <https://www.uoguelph.ca/chemistry/thomas/index>.
  - [17] J. H. Scofield, Theoretical photoionization cross sections from 1 to 1500 keV, Lawrence Livermore Laboratory report UCRL-51326 (1973), 10.2172/4545040.

- [18] Yong-Ki Kim, Self-consistent-field theory for closed-shell atoms, *Phys. Rev.* **154**, 17 (1967).
- [19] F. C. Smith and W. R. Johnson, Relativistic self-consistent fields with exchange, *Phys. Rev.* **160**, 136 (1967).
- [20] Riccardo Catena, Timon Emken, Nicola A. Spaldin, and Walter Tarinto, Atomic responses to general dark matter-electron interactions, *Phys. Rev. Res.* **2**, 033195 (2020).
- [21] P. Agnes *et al.* (DarkSide Collaboration), Constraints on Sub-GeV Dark-Matter Electron Scattering from the DarkSide-50 Experiment, *Phys. Rev. Lett.* **121**, 111303 (2018).